MAGNETISM
AND FERROELECTRICITY

Heat Capacity of the PbFe$_{1/2}$Ta$_{1/2}$O$_3$ Perovskite-Like Compound

M. V. Gorev*, I. N. Flerov*, V. S. Bondarev*, Ph. Sciau**, and A. G. Lehmann***

*Kirensky Institute of Physics, Siberian Division, Russian Academy of Sciences,
Akademgorodok, Krasnoyarsk, 660036 Russia
e-mail: gorev@iph.krasn.ru
**CEMES-CNRS, 29 Rue Jeanne Marvig, Toulouse, 31055 France
***Instituto Nazionale di Fisica della Materia (INFM) e Dipartimento di Fisica, Monserrato (Cagliari), 090124 Italy
Received July 8, 2003

Abstract—The heat capacity $C_p(T)$ of the complex perovskite PbFe$_{1/2}$Ta$_{1/2}$O$_3$ has been studied using adiabatic calorimetry in the temperature range 150–370 K. Three diffuse anomalies in $C_p(T)$ are found to exist at temperatures $T_d \approx 350$ K, $T_m \approx 250$–300 K, and $T_c \approx 205$ K. The anomalous and the lattice contribution to the heat capacity are separated, and the change in the entropy is determined. The results of the study are discussed jointly with the data on the structure and physical properties of the compound. © *2004 MAIK "Nauka/Interperiodica".*

1. INTRODUCTION

Double perovskites of type 1 : 1, with the general formula Pb$B_{1/2}^{3+}B_{1/2}^{5+}$ O$_3$, are classical model objects for the investigation of ferroelectrics–relaxors. Their properties can vary considerably without changing the chemical composition as a result of a variation in the ordering of the B^{3+} and B^{5+} ions over equivalent positions in the lattice [1, 2]. Highly ordered perovskites undergo ferroelectric or antiferroelectric phase transitions, whereas in the disordered state they exhibit properties characteristic of relaxors [2], namely, an anomaly in the dielectric permittivity ε broadened over a wide temperature interval and pronounced dependences of the temperature of its maximum (T_m) and of the magnitude of the maximum (ε_m) on the measuring field frequency.

The PbFe$_{1/2}$Ta$_{1/2}$O$_3$ compound (PFT) was first synthesized in the form of a ceramic and studied in [3]. It was found that the PFT has cubic symmetry $Pm3m$ at room temperature and that the Fe^{3+} and Ta^{5+} ions are distributed randomly over the B positions of the perovskite lattice. The cubic symmetry of the compound at room temperature was confirmed in subsequent x-ray measurements performed on single crystals [4].

The change in the PFT symmetry over a broad temperature range was studied by x-ray diffraction on single crystals [5–7]. Two phase transitions, at 270 and 220 K, were identified. The high-temperature phase, which is stable for $T > 270$ K, is paraelectric and optically uniaxial, despite its (pseudo)cubic symmetry. At 350 K, the symmetry of the compound was refined in space group $Pm3m$. The compound is characterized by a strong anisotropy in the oxygen thermal vibration parameters and by positional disorder or a strong anharmonicity in the thermal motion of the lead ions [6]. The

intermediate phase ($270 > T > 220$ K) was identified as tetragonal ($P4mm$). Within the interval $220 > T > 200$ K, the tetragonal phase coexists with the monoclinic phase. Below 200 K, only the monoclinic phase (Cm) is stable. The isostructural compound PbFe$_{1/2}$Nb$_{1/2}$O$_3$ (PFN) was also observed to undergo the cubic $\longrightarrow$ tetragonal $\longrightarrow$ monoclinic phase sequence [8].

The two low-temperature distorted phases were refined by the Rietveld method with the use of neutron and synchrotron experiments [5]. The distortions of the cubic phase are fairly small and were detected only as line broadenings in the diffraction pattern obtained with the angular resolution achievable with synchrotron radiation.

The low-temperature monoclinic phase Cm reveals large lead ion displacements along the [111] pseudocubic axis, so that the main lattice distortion, despite the monoclinic symmetry, is rhombohedral. The role of the monoclinic Cm phase, which couples the tetragonal and rhombohedral phases in complex lead-containing perovskites, is currently a subject of intense debate [9–11].

Small structural distortions in PFT and the difficulties encountered in establishing its symmetry were also pointed out in [12], where elastic neutron scattering studies were performed. These studies did not reveal any symmetry change within the temperature interval from 300 to 10 K. The data obtained by Rietveld refinement were interpreted in terms of the $R3m$ rhombohedral space group, which provided slightly better convergence as compared to the $Pm3m$ cubic lattice with positionally disordered lead ions [12].

There are numerous publications on the investigation of the dielectric properties of PFT [1, 13–15]. In addition to the diffuse, frequency-dependent maximum in ε(T) at $T_m \approx 243$ K, which is typical of relaxors, a small feature was observed in the behavior of ε(T) at a

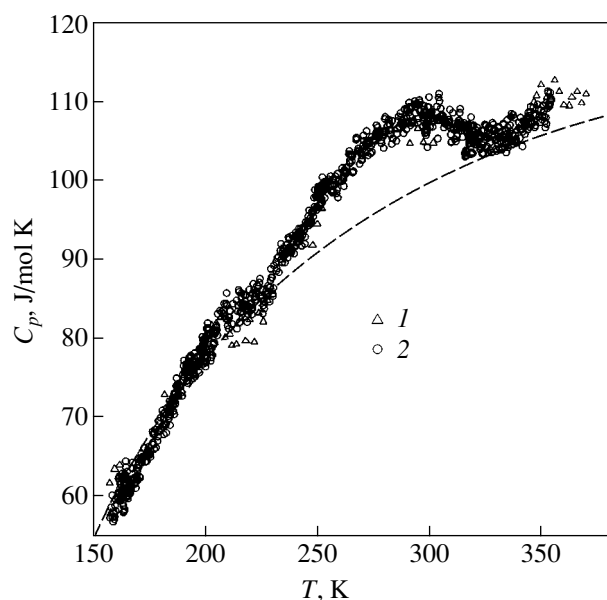**Fig. 1.** Temperature dependence of the specific heat of $PbFe_{1/2}Ta_{1/2}O_3$ obtained by (*1*) discrete heating and (*2*) continuous heating. Dashed line plots the lattice specific heat.

temperature T_{ip} [15], which is 30–40 K lower than T_m. Below this temperature, the frequency dispersion of ε is considerably weaker than that seen at higher temperatures [15]. This behavior is similar to that observed in $PbSc_{1/2}Ta_{1/2}O_3$ and $PbSc_{1/2}Nb_{1/2}O_3$ at the spontaneous transition from the relaxor to normal ferroelectric state [16].

To the best of our knowledge, spontaneous polarization in PFT was studied only in [14] along the [100] direction in electric fields of up to 8 kV/cm. The spontaneous polarization exists even above 300 K and reaches 28 $\mu C/cm^2$ at liquid-nitrogen temperature.

Birefringence Δn was observed in PFT in the range from 20 K up to the first-order phase transition temperature of 210 K [17]. Above 210 K, Δn is small and attains levels characteristic of growth defects as the temperature is increased [17].

As seen from this brief overview, the results obtained in various studies of PFT and their interpretations are more often than not at odds with one another. Despite the large number of diverse studies performed, many features in the behavior of PFT remain unclear.

Here, we report on a study of the heat capacity and thermodynamic parameters of PFT in order to obtain additional information on the changes in the energy characteristics that can take place in the elastic and electrical subsystems of PFT.

2. SAMPLE AND MEASUREMENT TECHNIQUES

The calorimetric measurements were performed on a sample studied earlier by neutron diffraction [5].

The PFT crystals were grown from a solution of the starting oxides in a PbO melt using the technique proposed in [18]. The remainder of the PbO melt was removed by rinsing the crystals in 30 wt % nitric acid. The grown crystals, having the pyrochlore structure, were sorted by hand in polarized light under a microscope. The PFT crystals selected in this way were ground. To reduce the strains created by grinding, the powders thus obtained were annealed for several hours at a temperature of about 850 K. After the annealing, the material was subjected to x-ray diffraction analysis, which showed the sample to be free of foreign phases and to produce clear and narrow Bragg reflections.

The heat capacity was studied in the temperature interval 100–370 K using adiabatic calorimetry, which made it possible to obtain absolute values of the heat capacity with a high accuracy. The sample ground to powder was placed in an indium container made airtight in a helium environment. Helium was employed as a heat-exchange gas to equalize the temperature over the sample. The mass of the sample was ~1 g, and the mass of the container was 9.8 g. Measurements were performed using the traditional technique of discrete heating and also in an automated regime under continuous heating with a variation in temperature at a rate $dT/dt \approx (2-3) \times 10^{-1}$ K min^{-1}. The experiment yielded the total heat capacity of the sample and the container. The heat capacity of the container was measured in a separate experiment. The accuracy with which the total heat capacity could be determined depends on the actual heating technique employed and is (0.1–0.5)%.

3. RESULTS OF THE STUDIES

Figure 1 displays the temperature dependences of the PFT specific heat obtained using the methods of discrete and continuous heating. The scatter of experimental points about the smoothing curve does not exceed 2%. The fact that this error is slightly larger than usual should be attributed to the heat capacity of the sample making up only a small fraction (about 10%) of the total heat capacity of the container plus sample system.

The analysis of the heat capacity should take into account the anharmonic contributions resulting in a difference between the isobaric (C_p) and isochoric (C_V) specific heats. The volume expansion coefficient estimated for the temperature range from 300 to 700 K from data on the temperature dependence of the cubic cell parameter varies from 9×10^{-6} to 35×10^{-6} K^{-1}. To the best of our knowledge, there are no data on the compressibility of PFT. We used data from [19] obtained in a study of the effect of pressure on the unit cell parameters of $PbZr_{1/2}Ti_{1/2}O_3$, which is related to PFT; its modulus of volume compressibility was measured to be 2.3×10^{-11} Pa^{-1}. Using these data, the anharmonic contribution to the specific heat was found to be ≤ 1 J/mol K below 700 K. Because this small quantity is within the experimental error, we disregarded the difference between C_p and C_V in the subsequent analysis. The

smallness of the anharmonic contribution is due to the comparatively small thermal expansion coefficient.

The lattice heat capacity C_L can be derived from the general relation

$$C_L = (\partial E/\partial T) = \frac{\partial}{\partial T}\left(\int d\omega G(\omega)n(\omega)\hbar\omega\right), \quad (1)$$

where E is the internal energy of the system, $n(\omega)$ is the Bose–Einstein distribution function, and $G(\omega)$ is the density of vibrational states. The density-of-states function $G(\omega)$ over the whole frequency range is, as a rule, unknown for fairly complex crystals. For this reason, the temperature dependence of heat capacity is calculated using a simplified approach. In most cases, in order to analyze the temperature dependence of the heat capacity and to separate the lattice and anomalous contributions, a simple model is used in which the lattice heat capacity of a compound is approximated by a combination of the Debye and Einstein functions. It is this approach that we used in the case with PFT. In the temperature range of interest to us, the heat capacity is only weakly sensitive to fine details in the vibration spectrum, which validates our separation of the lattice contribution.

The anomalous component of the specific heat $\Delta C_p = C_p - C_L$ is shown in Fig. 2. The maximum value of ΔC_p is 11 J/mol K, or ~10% of the lattice specific heat. The $\Delta C_p(T)$ relation clearly exhibits three regions of anomalous behavior, namely, near $T_1 \approx 350$ K, $T_2 \approx$ 250–300 K, and $T_3 \approx 205$ K.

The change in specific entropy associated with the anomalous behavior of the heat capacity can be calculated as $\Delta S(T) = \int_{100}^{T}\frac{\Delta C_p}{T}dT$; this quantity is plotted in Fig. 3 and constitutes 3.7 J/mol K.

4. DISCUSSION AND CONCLUSIONS

The heat capacity anomalies coincide in temperature with the anomalous behavior of the structural, magnetic, optical, and dielectric properties.

In the temperature region near 350 K, earlier studies revealed deviations of the lattice parameters from their regular course [4] and of the $\varepsilon(T)$ behavior from the Curie–Weiss law [13, 15]. The anomalous behavior of the heat capacity over the temperature range 250–300 K correlates with that of the dielectric permittivity [13, 15] and of the interplanar distance d_{222} [7]. Near T_3, jumps in the birefringence [17] and in d_{222} [7] and specific features in the $\varepsilon(T)$ behavior [13, 15] were observed. The fairly large scatter of experimental points in the interval 160–170 K can probably be assigned to the transition of PFT to the antiferromagnetic state [14].

On the one hand, our calorimetric results agree to a certain extent with the data reported in [4–7]. The PFT can be expected to undergo the following sequence of
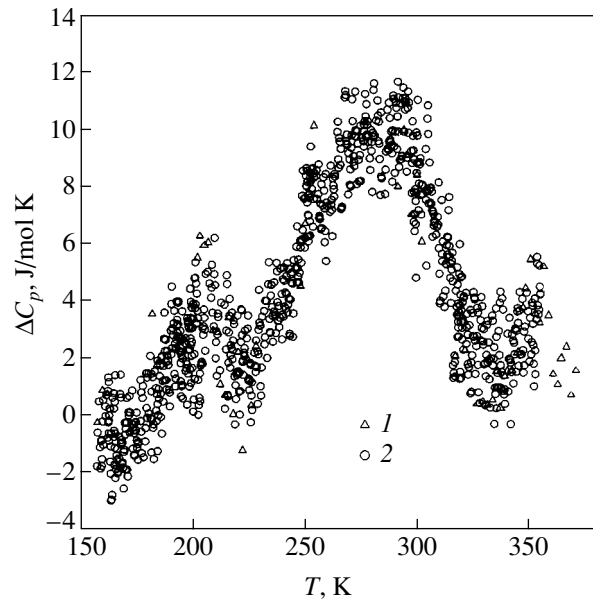
Fig. 2. Temperature dependence of the anomalous component of the specific heat of PbFe$_{1/2}$Ta$_{1/2}$O$_3$ obtained by (*1*) discrete heating and (*2*) continuous heating.

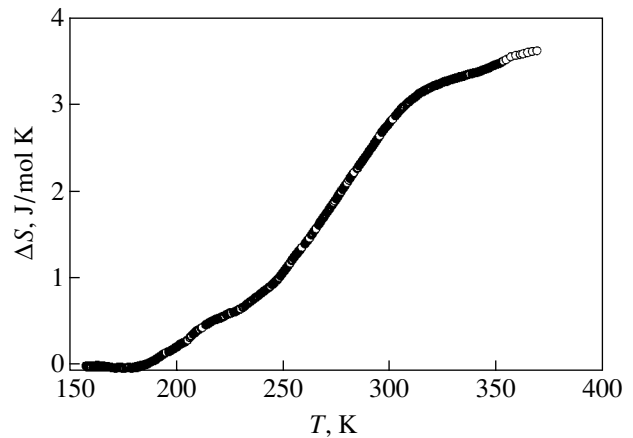**Fig. 3.** Temperature dependence of the anomalous contribution to the specific entropy of PbFe$_{1/2}$Ta$_{1/2}$O$_3$.

structural transformations with decreasing temperature: cubic paraelectric (*Pm3m*, $T > 350$ K) ⟶ tetragonal antiferroelectric ($350 < T < 270$ K) ⟶ tetragonal ferroelectric (*P4mm*, $270 > T > 205$ K) ⟶ monoclinic ferroelectric (*Cm*, $205 > T > 160$ K) ⟶ antiferromagnetic phase ($T < 160$ K).

On the other hand, the diffuseness of the heat capacity anomalies, the noticeable dispersion of ε, and its clearly pronounced relaxor behavior [13, 15] may signal a certain structural inhomogeneity of this compound and permit interpretation of our data from other standpoints as well.

In double perovskites of the A$B'_{1/2}B''_{1/2}$O$_3$ composition, the B' and B'' cations can either occupy positions

at the centers of octahedra in a random manner or alternate in adjacent octahedra. Such compositional ordering gives rise to unit cell doubling and the formation of a superstructure. The degree of compositional ordering is quantified by a parameter *s*, which is unity in the completely ordered state and zero in the state of disorder. Compositional ordering occurs under cooling as a result of a phase transition and consists in a diffusive redistribution of the ions [20]. The temperature of transition to the compositionally ordered state is determined by the difference in size and valency between the *B*' and *B*'' ions. For low transition temperatures, the disordered or partially ordered state can also persist at fairly low temperatures, where diffusion is practically impossible.

Present-day relaxor models attach a significant role to the existence of compositionally ordered regions randomly distributed in a disordered crystal matrix. Such nanoscale regions have been revealed using various methods in the model relaxors $PbMg_{1/3}Nb_{2/3}O_3$ and $PbSc_{1/2}Ta_{1/2}O_3$. The existence of such regions in PFT could be experimentally verified by detecting weak superstructural reflections in x-ray diffraction studies of the crystals [13] and by investigating antiferromagnetic ordering [14, 21]. In the latter case, the Néel temperatures (T_N is 143 K for the ceramics studied in [21] and 180 K for the crystal [14]) lie between the values calculated for the completely ordered and totally disordered states, which is interpreted as an argument for partial compositional ordering of the ions, because T_N depends strongly on the number of magnetically active ions in adjacent cells [22]. The degree of ordering substantially depends on the method of preparation and thermal history of a sample. It is also pointed out that the ordering process is most likely to be of a local nature; i.e., the crystal contains mesoscopic regions with various degrees of order. The x-ray superstructural reflections are very weak because of the scattering powers of ordering ions being similar and because of the smallness of the ordered regions, which diffuses the reflections.

The existence of ordered and disordered regions and the variation in their symmetry with temperature could make interpretation of structural data difficult.

Compositional nonuniformity of a material generates random local electric fields and mechanical strains, which play a significant role in the formation of polar nanoregions and the relaxor properties of perovskites [2, 23]. The correlation length of polar clusters is fairly small, such that no macroscopic polarization appears in the sample. In PFT, these polar regions possibly appear at the Burns temperature $T_d \approx 350$ K. At this temperature, the dielectric permittivity begins to deviate from the Curie–Weiss law and anomalies are observed in the behavior of the unit cell parameter $a(T)$ and of the heat capacity. Note that the anomalous behavior of $a(T)$ in this temperature region is associated with the formation of polar regions and the deviation of the rms polarization from zero [24].

The entropy change in PFT is ~0.4*R*, which indicates that an important role is played in the formation of polar nanoregions by order–disorder-type processes, which are related, as in other lead-containing perovskites, with positional ordering of lead ions in interoctahedral cavities below the Burns temperature. In ordered regions with Fe^{3+} and Ta^{5+} ions alternating along the cubic cell edges and with $Fm\bar{3}m$ symmetry for $T > T_d$, lead can turn out to be distributed over four positions displaced from the center of the cavity along the $[111]_c$-type directions. Lead ion ordering should bring about a change in the entropy $\Delta S = R\ln(4)$ if the whole crystal has undergone the transition. The experimental value of ΔS is only 3.7 J/mol K, or ~30% of the maximum possible value, which is close to the volume fraction of ordered regions derived from structural [13] and magnetic [14] studies.

To describe the behavior of relaxors containing interacting polar nanoregions at temperatures $T < T_d$, a spherical random-bond–random-field model was proposed in [25]. The model considers a system of coupled, randomly reorienting nanoclusters in the presence of random electric fields. It is assumed that both random interactions (or bonds) and random electric fields have Gaussian distributions [25].

In the absence of an external field ($E = 0$), there are two sets of solutions. One of them, $P = 0$, $q \neq 0$, corresponds to a phase without long-range order (spherical glass). The other solution, $P \neq 0$, $q \neq 0$, describes a phase with long-range order (ferroelectric phase).

For $J_0 < \sqrt{J^2 + \Delta}$ (J_0 is the average interaction, J is the standard deviation of the interaction, and Δ is the variance of the field; the mean field is equal to zero), long-range order does not arise and the system resides in the spherical glass (SG) state down to 0 K. If $\Delta = 0$, as is the case with magnetic spin glasses, a transition from the paraelectric to the SG phase occurs at $T_f = J/k$. For $\Delta \neq 0$ and $\Delta \ll J^2$, there is no longer a clearly defined phase transition, but the dielectric permittivity [25] and the heat capacity [26] pass through a maximum at $T_m = T_f \approx (\sqrt{J^2 + \Delta})/k$. For $J_0 > \sqrt{J^2 + \Delta}$, long-range order can arise and a phase transition to a nonuniform ferroelectric phase can take place at $T_c = J_0(1 - \Delta/(J_0^2 - J^2))/k < T_m$.

Thus, the temperatures of the three heat capacity anomalies observed in PFT can, in our opinion, be identified with the temperatures T_d (the temperature of formation of polar regions), T_m (the temperature of the maximum permittivity), and T_c (the temperature of the spontaneous transition to the ferroelectric state).

ACKNOWLEDGMENTS

REFERENCES

1. I. P. Raevskiĭ, V. V. Eremkin, V. G. Smotrakov, *et al.*, in *Proceedings of International Seminar on Order, Disorder, and Properties of Oxides* (Sochi, 2001), p. 246.

2. E. L. Cross, Ferroelectrics **151**, 305 (1994).

3. G. A. Smolenskiĭ, A. I. Agranovskaya, and V. A. Isupov, Fiz. Tverd. Tela (Leningrad) **1** (6), 990 (1959) [Sov. Phys. Solid State **1**, 907 (1959)].

4. Yu. Venevtsev, N. E. Skorohodov, and V. V. Chechkin, Ferroelectrics **137** (1), 57 (1992).

5. N. Lampis, Ph. Sciau, and A. G. Lehmann, J. Phys.: Condens. Matter **12** (11), 2367 (2000).

6. A. G. Lehmann, F. Kubel, and H. Schmid, J. Phys.: Condens. Matter **9** (39), 8201 (1997).

7. A. G. Lehmann and Ph. Sciau, J. Phys.: Condens. Matter **11** (5), 1235 (1999).

8. W. Bonny, M. Bonin, Ph. Sciau, *et al.*, Solid State Commun. **102**, 347 (1997).

9. R. Guo, E. L. Cross, S. E. Park, *et al.*, Phys. Rev. Lett. **84** (23), 5423 (2000).

10. B. Noheda, J. A. Gonzalo, E. L. Cross, *et al.*, Phys. Rev. B **61** (13), 8687 (2000).

11. B. Noheda, D. E. Cox, G. Shirane, *et al.*, Phys. Rev. B **63**, 014103 (2001).

12. S. A. Ivanov, S. Eriksson, N. W. Thomas, *et al.*, J. Phys.: Condens. Matter **13** (1), 25 (2001).

13. I. P. Raevskiĭ, V. V. Eremkin, V. G. Smotrakov, *et al.*, Kristallografiya **47** (6), 1076 (2002) [Crystallogr. Rep. **47**, 1007 (2002)].

14. S. Nomura, H. Takabayashi, and T. Nakagawa, Jpn. J. Appl. Phys. **7** (6), 600 (1968).

15. I. P. Raevski, S. A. Prosandeev, U. Waghmare, *et al.*, cond-mat/0208116 (2002).

16. F. Chu, I. M. Reaney, and N. Setter, Ferroelectrics **151**, 343 (1994).

17. W. Brixel, J. P. Rivera, and H. Schmid, Ferroelectrics **55**, 181 (1984).

18. W. Brixel, R. Boutellier, and H. Schmid, J. Cryst. Growth **82**, 396 (1987).

19. J. Roquette, J. Haines, V. Bornand, *et al.*, Phys. Rev. B **65** (21), 214102 (2002).

20. A. A. Bokov and I. P. Raevski, Ferroelectrics **144**, 147 (1993).

21. M. V. Plotnikov, K. P. Mitrofanov, V. S. Shpinel', and Yu. N. Venevtsev, *Barium Titanate* (Nauka, Moscow, 1973), p. 156.

22. Yu. N. Venevtsev, V. V. Gagulin, and V. N. Lyubimov, *Ferroelectrics* (Nauka, Moscow, 1982).

23. H. Qian and A. Bursill, Int. J. Mod. Phys. B **10**, 2007 (1996).

24. G. A. Samara, J. Phys.: Condens. Matter **15**, 367 (2003).

25. R. Pirc and R. Blinc, Phys. Rev. B **60** (19), 13470 (1999).

26. M. V. Gorev, I. N. Flerov, V. S. Bondarev, and Ph. Sciau, Zh. Éksp. Teor. Fiz. **123** (3), 599 (2003) [JETP **96**, 531 (2003)].

Translated by G. Skrebtsov